

THE DESIGN OF THE ARGONNE DOUBLE-SIDED MICROTRON\*

Tat K. Khoe, Yanglai Cho, Roy J. Holt,  
Harold E. Jackson, and George S. Mavrogenes  
Argonne National Laboratory  
Argonne, Illinois 60439

Summary

The design study of a double-sided microtron is presented. The result of beam optic calculations in several sector magnet configurations is described. Current limitation by beam backup is discussed.

Introduction

The study of a 0.5-2.0 GeV, 100% duty cycle electron accelerator was initiated at Argonne in 1979. Several schemes for achieving the 100% duty cycle have been explored. The results of the study of two accelerator concepts have been described in a detailed report<sup>1</sup> and a summary paper.<sup>2</sup> The scheme, utilizing the double-sided microtron, has been adopted for further study because of its lower capital cost and better beam quality.

General Description

A schematic layout of the accelerator system is given in Fig. 1. The injector is a 5 MeV CW electron linac. The transport and matching systems are not shown in this figure. The electron beam enters the microtron through a septum magnet and the last magnet of the chicane system (see Fig. 1). After passing through the linac and the radial-focusing quadrupole, the beam enters one of the four 90° sector magnets. Note that with an energy gain of 25 MeV per linac, the lowest energy of the orbits in the sector magnets is 30 MeV. The two linacs in the long straight sections are identical. Variable energy extraction is achieved by a movable septum magnet in the short straight section, followed by a fixed septum magnet in the drift space between the sector magnet and the linac. The design objectives are summarized in Table 1.

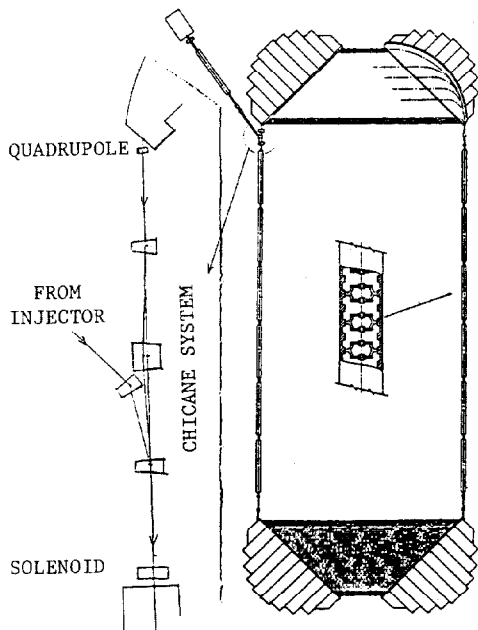


Fig. 1. Schematic Layout of the Microtron

Table 1

Beam Energy	0.5 - 2.0 GeV
Beam Current	100 $\mu$ A per beam
Number of Beams	3
Duty Cycle	100%
Energy Spread	$< \pm 200$ keV
Transverse Emittance	$< 0.2\pi$ mm-mrad

The splitting into three beams utilizes a combination of an accelerating cavity with resonant frequency equal to one-third of the linac RF frequency and a bending magnet.

Injector

The required performance parameters of the injection linac are given in the following table.

Table 2

Beam Energy	5 MeV
Beam Current	$> 300$ $\mu$ A
Duty Cycle	100%
Transverse Emittance	$\leq 1\pi$ mm-mrad
Bunch Width	$\approx \pm 1^\circ$
Energy Spread	$\approx \pm 50$ keV

Comparing this table with Table 1, we see that during the acceleration in the microtron, a transverse phase space dilution factor of 40 can be tolerated. In the longitudinal motion, the dilution factor must be less than four. A detailed study of the injection system is underway.

Accelerating System

The accelerating system consists of two identical 25 MeV CW linacs. The cavities will be of the disk-and-washer type<sup>3</sup> operated in the  $\pi/2$  mode. It has the advantage of high effective shunt impedance and strong cell-to-cell coupling. Each linac is divided into 3 m long sections with solenoid focusing between the sections. The field of these solenoids is constant and chosen such that the phase advance of the transverse motion would be 90° per focusing period if the energy of the electrons remains 5 MeV. Table 3 summarizes the performance specifications.

Table 3

RF Frequency	2400 MHz
Duty Cycle	100%
Accelerating Field	1.4 MV/m
Energy Gain per Linac	25 MeV
Synchronous Phase	90°
Effective Shunt Impedance (estimate)	85 $\Omega$ /m
RF Losses	$\sim 830$ kW
Strength of focusing solenoid	
$\int_{-\infty}^{\infty} B^2 dl$	$\approx 7.5 \times 10^{-4} T^2 - m$

The phase velocity of the linac structure is equal to the velocity of light. Since the electron velocity is slightly smaller than the velocity of light, the

\*Work supported by the U.S. Department of Energy.

phase of the center of the bunch slips during the acceleration in the linac. The phase slip is given by

$$\sin \phi_2 - \sin \phi_1 = \frac{2\pi}{eE\lambda} \left[ \sqrt{W_2^2 - W_0^2} - \sqrt{W_1^2 - W_0^2} - W_2 + W_1 \right] \quad (1)$$

where  $\phi_1$  and  $\phi_2$  are the phase of the bunch, respectively, at the entrance and exit of the linac,  $W_1$  and  $W_2$  are the corresponding energies,  $W_0 = 0.511$  MeV, and  $eE$  is the maximum energy gain per unit length. We see from Eq. (1) that the phase slip is only large for the acceleration from 5 MeV to 30 MeV. The choice of  $\phi_1$  is determined by the longitudinal phase space matching requirement. This matching condition is satisfied for  $W_1 = 5$  MeV,  $\phi_1 = -18^\circ$ ,  $W_2 = 30$  MeV, and  $\phi_2 = +23^\circ$  (see Fig. 2). For the acceleration from 30 MeV to 55 MeV, the phase slip is approximately  $4^\circ$ .

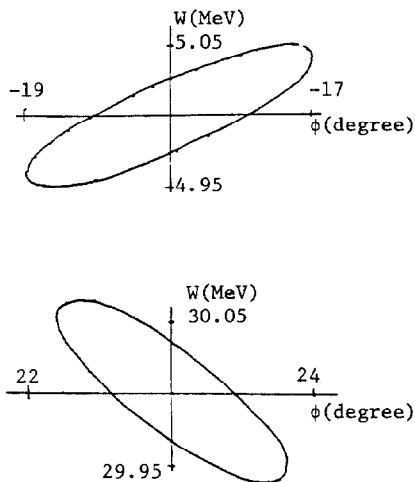


Fig. 2. Longitudinal Phase Space Ellipses

#### Beam Dynamics and Magnet Design

In the original double-sided microtron, the  $45^\circ$  entrance and exit edge angles are both defocusing in the vertical direction (see Fig. 3). The result is a considerable problem of beam optics at low energies, where the electron trajectories are mainly in the fringing fields. To study this problem, a partial prototype magnet has been constructed. This magnet represents a portion of the sector magnet containing the trajectories of the first six passes. The pole edge configuration that has satisfactory beam optical properties is shown in Fig. 4. The compensating quadrupole singlet is x-focusing.

For the double-sided microtron, the synchronism condition is given by the relation:

$$\frac{(\pi - 2)\Delta W}{eBc} = \frac{n}{2} \lambda \quad (2)$$

where  $\Delta W$  is the energy gain per turn,  $n$  is the increase of the harmonic number per turn,  $\lambda$  is the RF wave length, and  $B$  is the sector magnet field strength. This field is assumed to be uniform and that it changes abruptly from zero to the value  $B$  at the edges (hard

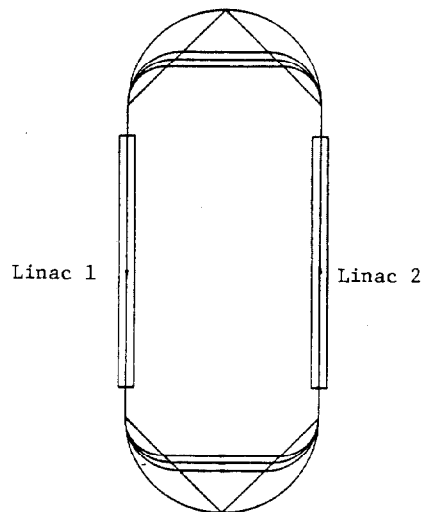


Fig. 3. Original Design

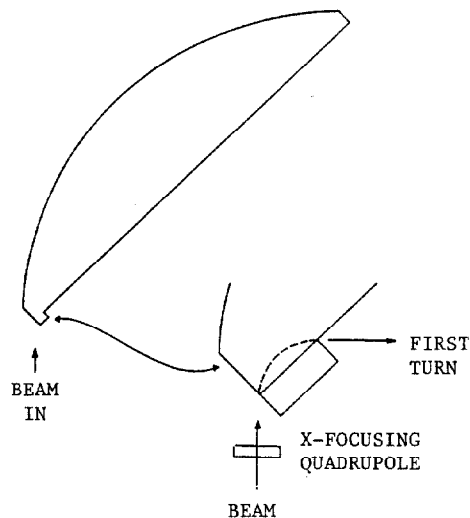


Fig. 4. 2-GeV Microtron-Sector Magnet Field Region

edge). The actual magnet has extended fringe fields (soft edge) resulting in a displacement of the orbits from the corresponding hard edge case. Since, in the long straight sections the equilibrium orbits (e.o.) have to coincide with the axis of the linac, the e.o. in the short straight section are not only displaced but the bending angles become less than  $90^\circ$ . The increase of the orbit length because of the soft edges are negligible except for the lowest energy orbits. However, the change in the bending angles must be corrected either by pole face windings and/or pole edge shims. Transverse focusing is mainly achieved with quadrupoles in the short straight sections. The locations and strengths of the quadrupoles are chosen such that the following conditions are satisfied:

1. The trajectories in the long straight sections are dispersion-free.
2. The beam envelope has a waist at the midpoints of the short straight sections.
3. The system has mirror symmetry about these midpoints.

Conditions 2 and 3 will give matched transverse phase space ellipses from the exit of one linac to the

entrance of the other linac. Table 4 shows some magnet and orbit parameters.

Table 4

Bending Magnet Field Strength	1.523 T
Magnet Gap Height	3.5 cm
Maximum Orbit Radius	438 cm
Orbit Separation	10.95 cm
Maximum Number of Recirculation	40
First Turn Harmonic Number	530
Increase of Harmonic Number per Turn	2
Length of Long Straight Section	21.72 m
Maximum Length of Short Straight Section	11.17 m
Strength of Compensating Quadrupole	1 T/m-m

#### Beam Breakup

It has been known in RF separators that the lowest order deflecting force at  $v_{ph} = c$  is constant in magnitude and direction over the aperture of the cavity. This force gives a deflection inversely proportional to the energy of the electron. Therefore, the trajectories in the linac of the higher energy bunches are mainly determined by the quadrupoles in the short straight sections. On the other hand, the deflecting field is excited by all bunches independent of the energy. The amount of the excitation is proportional to the sum of the displacement of the bunches from the cavity axis. Therefore, reducing the sum of these displacements will increase the beam breakup threshold current. If it turns out that the beam breakup can be attributed to a single mode, the use of an active damping system will be contemplated. Assuming that, either by adjusting the strength of the quadrupoles in the short straight sections and/or by using an active damping system, the sum of the transverse displacement of the recirculated beam can be made negligible, a threshold current in excess of 300  $\mu$ A can be obtained.

#### Discussion

The double-sided microtron proposed here offers considerable flexibility. Energy variation over a series of discrete energies can be accomplished by adjusting the location of a septum magnet of constant strength. Combining subharmonic chopping at the injector with subharmonic beam splitting (as in the NBS-LASL Microtron design<sup>4</sup>) satisfies the specific objective of allowing independent variation of currents of each split beam. A system allowing independent control of the energies of the three beams is under study. This method used subharmonic modulation of the bunch phases at injection. This phase difference becomes energy difference in the linac and orbit displacement in the short straight sections. A similar system has been suggested for the MIT-BATES recirculator.<sup>5</sup>

#### References

1. Y. Cho, R.J. Holt, H.E. Jackson, T.K. Khoe, and G.S. Mavrogenes, *Study of a National 2-GeV Continuous Beam Electron Accelerator*, Argonne National Laboratory Report ANL-PHY-79-2 (Revised) (1979).
2. Y. Cho, R.J. Holt, H.E. Jackson, T.K. Khoe, and G.S. Mavrogenes, Proc. 11th Int'l. Conf. on High Energy Accelerators, CERN (1980).
3. S.O. Schriber, *High-Beta Linac Structure*, Proc. 1979 Linear Accelerator Conf., Montauk, N.Y.
4. S. Penner and L.M. Young, *NBS-LASL Microtron Design* (unpublished).
5. C.P. Sargent, J. Flanz, and G. Franklin, *MIT-BATES 2-GeV CW Recirculator* (unpublished).